High-pressure x-ray diffraction study of CeO_2 to 70 GPa and pressure-induced phase transformation from the fluorite structure

Steven J. Duclos, Yogesh K. Vohra, and Arthur L. Ruoff
Department of Materials Science and Engineering, Cornell University, Ithaca, New York 14853

A. Jayaraman and G. P. Espinosa
AT&T Bell Laboratories, Murray Hill, New Jersey 07974
(Received 7 April 1988)

The crystal structure of CeO_2 has been investigated to 70 GPa using energy dispersive x-ray diffraction in a diamond-anvil cell. At 31.5±1.0 GPa the fluorite phase transforms, on loading, to an orthorhombic α-$PbCl_2$-like structure of space group *Pnam*, with a 7.5%±0.7% increase in density. The cubic fluorite phase has a bulk modulus $B_0 = 230 \pm 10$ GPa with an assumed pressure derivative of $B_0' = 4.00$. The α-$PbCl_2$-type structure seems to be the stable high-pressure phase in the case of the group-IV*B*, lanthanide, and actinide fluorite-type dioxides, independent of metal-ion size, at reduced volumes less than 0.89±0.01.

INTRODUCTION

Most cubic fluorite structure difluorides, including CaF_2, CdF_2, SrF_2, BaF_2, MnF_2, PbF_2, and EuF_2,[1-7] have been shown to transform to the α-$PbCl_2$-type structure at pressures below 10 GPa. A similar transition occurs in the distorted fluorite structure oxyfluorides GdOF, EuOF, SmOF, NdOF, PrOF, and ErOF (Ref. 8) quenched from approximately 1000 °C and 4–9 GPa. In the fluorite-type dioxides the picture is considerably less clear. Quenching experiments on ZrO_2, HfO_2, and TbO_2 (Refs. 9 and 10) and *in situ* room-temperature experiments on ZrO_2 (Refs. 11,12) have shown the α-$PbCl_2$ (or a distorted form) stable above 15–20 GPa. These are the dioxides with the smallest metal-ion radii that are known to crystallize in the fluoritelike structure. Quenching experiments on PrO_2, CeO_2, UO_2, and ThO_2 (Ref. 10) failed to show a high-pressure α-$PbCl_2$ form, and Liu has argued[10,23] that this transition, if it exists at all, should occur at lower pressures in these larger metal-ion dioxides. Preliminary *in situ* results on cubic fluorite structure UO_2,[14,15] however, have indicated the possibility of a transition to the α-$PbCl_2$ structure around 35 GPa. Further, recent high-pressure Raman studies on CeO_2 (Ref. 16) and ThO_2 (Ref. 17) have indicated that transitions occur at 31 and 30 GPa, respectively, and that their high-pressure spectra would be consistent with the lower-symmetry α-$PbCl_2$ structure.

The question of the stability of the fluorite structure under pressure is of much interest from the solid-state chemistry point of view as there is a series of group-IV, lanthanide, and actinide[18] metal dioxides with a range of metal-ion sizes. Further, the question is of geophysical interest as SiO_2 may go through a fluorite and post fluorite structure at the pressure- temperature conditions prevailing in the deeper mantle region. Therefore, we have studied this phase transition in CeO_2 with a high-intensity synchrotron x-ray diffraction experiment to 70 GPa to settle the structure of the high-pressure phase.

EXPERIMENT

The CeO_2 crystals used in this experiment were grown from $Li_2W_2O_7$ flux in a platinum crucible. The molten solution (starting materials: CeO_2, Li_2CO_3, WO_3) was held at a temperature of 1280 °C for 6 h, then cooled at a rate of 2.5 °C/h to 1000 °C at which point the crucible was cooled to room temperature in the furnace. These crystals are from the same batch used for earlier Raman scattering experiments.[16]

Diamonds with a 300-μm flat and no bevel were used in a gasketed diamond-anvil cell. Gasketing consisted of hardened spring steel 250 μm thick preindented to 40 μm. A hole 50 μm in diameter was packed with CeO_2 powder. Pressures were measured with the R_1 fluorescence shift of a centered $10\times15\times5$-μm^3 ruby chip (0.5wt % Cr^{3+}) using the calibration of Mao *et al.*[19] Throughout the experiment both R_1 and R_2 fluorescence lines were observed. Energy dispersive x-ray diffraction (EDXD) spectra were collected on the six-pole wiggler polychromatic beam line at the Cornell High Energy Synchrotron Source. Details of the experimental setup are given by Brister, Vohra, and Ruoff.[20] In this study 20–30 μm x-ray collimation was used. All spectra were obtained at room temperature (300 K).

RESULTS

Figure 1 shows x-ray spectra of CeO_2 at the extremes of pressure of this study. The atmospheric pressure spectrum, actually taken after release of pressure from 70 GPa, shows a pure cubic fluorite phase with $a_0 = 5.406 \pm 0.010$ Å, in agreement with the powder diffraction value of $a_0 = 5.411$ Å.[21] Therefore, any high-pressure phase is unquenchable at room temperature. On loading, new peaks of the high-pressure phase appeared between spectra at 30.6 and 32.5 GPa, in excellent agreement with the 31-GPa phase transition pressure observed in Raman studies by Kourouklis *et al.*[16] Complete trans-

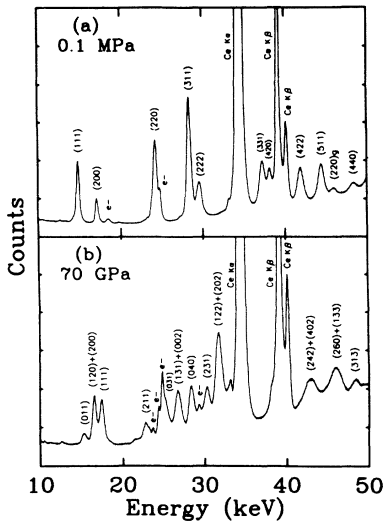

FIG. 1. Energy dispersive x-ray diffraction patterns of CeO_2 (a) in the cubic fluorite phase at ambient conditions after release of pressure and (b) in the *Pnam* phase at 70.0 GPa. Both spectra were taken on the CHESS wiggler beam line with critical energy 28 keV, and diffraction angle $\theta=7.71°$ ($Ed=46.23\pm0.03$ keV Å). Escape peaks from the Ge x-ray detector are labeled e^-, and gasket peaks are labeled $(hkl)g$.

TABLE I. Observed and calculated d spacings for CeO_2 in the *Pnam* phase at 70 GPa; $a=5.457$ Å, $b=6.521$ Å, $c=3.427$ Å. The average $|\Delta d/d|$ is 0.17%.

hkl	d_{obs} (Å)	d_{calc} (Å)	$\lvert\Delta d/d\rvert$ (%)
011	3.014	3.034	0.60
120	2.797	2.799	0.05
200	2.736	2.729	0.27
111	2.650	2.651	0.07
211	2.031	2.028	0.10
031	1.834	1.836	0.08
131	1.738	1.740	0.09
002	1.718	1.714	0.29
040	1.630	1.630	0.00
231	1.526	1.523	0.22
122	1.466	1.461	0.32
202	1.450	1.451	0.04
240	1.398	1.399	0.11
042	1.177	1.181	0.34
322	1.162	1.165	0.26
242	1.085	1.084	0.06
402	1.069	1.067	0.17
260	1.008	1.010	0.16
313	0.958	0.957	0.11

formation to the high-pressure phase did not occur until 38 GPa. This may be due to pressure gradients within the sample region, but the Raman studies of CeO_2 (Ref. 16) and studies on UO_2 (Refs. 14 and 15) indicate that the transition is sluggish.

The high-pressure phase of CeO_2 indexes well to an orthorhombic cell with $a=5.457$ Å, $b=6.521$ Å, $c=3.427$ Å, and four units of CeO_2 per unit cell. A comparison of the observed and calculated d spacings is shown in Table I. The extinctions for space group *Pnam* and atomic positions 4(c) or 8(d) [$(0kl)k+l=2n+1$, and $(h0l)h=2n+1$] are seen to be satisfied by the 19 observed peaks. In addition, the extinction of the (021) and (030) peaks is confirmed by a prominent absence of diffraction peaks near 20 keV [Fig. 1(b)]. The axial ratios $a/c=1.605\pm0.019$, and $b/c=1.897\pm0.004$ are well within the range of ratios observed in crystals of this space group at atmospheric pressure. Within the errors of this experiment no pressure dependence of these axial ratios was observed. Due to the low symmetry of the cell, several sets of peaks are separated by energies comparable to the system resolution as determined by the intrinsic Ge x-ray detector and geometrical broadening due to finite slit sizes. In these cases a least-squares deconvolution technique was used to extract the peak maxima. While we expect other less intense diffraction peaks in the range of d spacings covered by Table I, the success of the orthorhombic fit indicates that the peaks listed in the table are the most intense. Further, each peak listed is a relatively strong reflection in the *Pnam* powder pattern of α-$PbCl_2$.[21] The implications of the intensities of these peaks are discussed in the next section.

Figure 2 shows the equation of state (EOS) of CeO_2 to 70 GPa. A fit to the Birch first-order EOS (Ref. 22) of the cubic fluorite phase gives the bulk modulus $B_0=230\pm10$ GPa when the bulk modulus pressure derivative is constrained to $B_0'=4.00$. Although the bulk modulus of UO_2 is the same, 230±8 GPA,[14] the measured B_0' is 7±2, making UO_2 less compressible than CeO_2. A 7.5%±0.7% volume decrease accompanies the CeO_2 phase transition, and the high-pressure phase extrapolated back to atmospheric pressure is 9%±1% more dense than the equilibrium cubic fluorite structure. Therefore the orthorhombic structure observed at high pressures would, at atmospheric pressure, have $d_{120}=2.96$ Å and $d_{111}=2.80$ Å. These spacings match the two new lines ($d=2.966$ and 2.804 Å) observed by Liu[10] after CeO_2 was quenched from 20 GPa and 1000 °C.

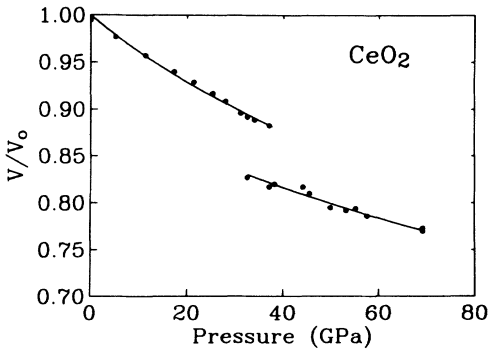

FIG. 2. The room-temperature equation of state of CeO_2. Solid curves are Birch first-order equation of state fits for the fluorite phase $B_0=230\pm10$ GPa, $B_0'=4.00$. The high-pressure phase has $B_0=304\pm25$ GPa, $B_0'=4.00$, and its fractional volume extrapolated back to atmospheric pressure is 0.91 ± 0.01.

If this indicates stability of quenched *Pnam* structure material, then at these temperatures this phase seems to appear at lower pressures than at room temperature, which is quite consistent from kinetic considerations. However, this would require the peculiar result that the phase is quenchable from high pressure at 1000 °C but not from high pressure at 23 °C. This may be an indication that this high-temperature and high-pressure phase of CeO_2 is different from the one observed in this study at room temperature. On the other hand, it is possible that because of the sluggishness of the transition small regions maintain the low-pressure structure even at 70 GPa, so on unloading there are nuclei present to ease the reverse transition. At high temperatures the transition should be complete so that when the temperature is lowered, and then the pressure, the phase formed at high pressure can be quenched (because no nuclei are present). Also, deformations present at room temperature but annealed at high temperature may contribute to the reverse transformation. It should be pointed out that similar quenching properties have been observed in CaF_2.[1] Further studies will be required to clarify this point.

During the x-ray experiment the CeO_2 powder became increasingly dark yellow-brown in transmission, most likely due to radiation damage. The Goldhammer-Herzfeld[23] criterion predicts a fractional volume of 0.56 for metallization, which would correspond to a pressure of approximately 400 GPa, if no further first-order phase transition occurs. Hence we do not attribute the above change in the transmission to any movement of the fundamental absorption edge to the visible region.

DISCUSSION

Our results have shown that CeO_2 transforms to an orthorhombic structure of the *Pnam* space group at 31.5 GPa. It has been suggested[10,13] that the large metal-ion dioxides might be transforming to a different structure (possibly δ-Ni_2Si) whereas the smaller ion dioxides are generally considered to transform to the α-$PbCl_2$-like structure at high pressure. Both δ-Ni_2Si and α-$PbCl_2$ structures belong to the *Pnam* space group and differ only in the six positional parameters of the 12 atoms at the 4(c) positions within the unit cell. These positional parameters will affect only the diffraction peak intensities. Since Ce has an x-ray scattering factor approximately 50 times that of O, the x-ray peak intensities will be determined predominantly by the Ce atom positions. The differences in the metal-atom positions in the α-$PbCl_2$ and δ-Ni_2Si structures are slight, less than 10% of the unit-cell edge. Calculated x-ray intensities of the two structures, therefore, do not differ significantly, especially for the well-separated large-*d* spacing lines. Due to possible orientational effects in this nonisotopic orthorhombic structure, it is not possible to assign intensities with the accuracy required to distinguish the two possibilities. Raman spectroscopy on powder samples has similar restrictions, and is insensitive to the positional parameters[4]. Further, there is no *a priori* reason to assume the positional parameters are those of either α-$PbCl_2$ or δ-Ni_2Si, and any general structure refinement is ruled out by these orientational effects. We point out, however, that comparing the axial ratios of materials crystallizing in *Pnam* structures at ambient conditions to those measured for CeO_2 at high pressures, as in Fig. 3, indicates that the postfluorite phase has atomic positions nearer to α-$PbCl_2$ than δ-Ni_2Si. The use of axial ratios to distinguish these two structures is discussed by Jeitschko.[24]

Raman spectroscopy has shown that the high-pressure phase of ThO_2 (above 30 GPa) has the same space group as that of CeO_2.[17] Also, the present x-ray work supports the preliminary conclusion[14,15] that UO_2 transforms to the orthorhombic *Pnam* space group at pressures above 35±3 GPa. An *in situ* room-temperature study[11] of ZrO_2 has shown that this phase becomes stable above 16 GPa, and was quenchable from 1000 °C and 10 GPa.[9] Also, HfO_2 was found to have this structure after quenching from 1000 °C and 15 GPa.[9] Therefore, dioxides covering the entire range of metal-ion sizes have been shown to transform from the fluorite-type structure to an orthorhombic structure of space group *Pnam*, with the exception of PoO_2, the largest metal-ion dioxide crystallizing in the fluorite structure, which has not been studied *in situ* at high pressures.

As shown in Table II, the transition pressure generally increases with increasing metal-ion size, which is inconsistent with the general trend observed for transition pressures among related materials.[13] Further examination shows that at room temperature the fluorite-type structure becomes unstable at a reduced volume $V_t/V_0 = 0.89 \pm 0.01$, where V_0 and V_t are the initial and final volumes, respectively, of this fluorite-type structure preceding the *Pnam* structure. Thus, the lower compressibility of the large metal-ion dioxides may account for their higher transition pressures. It has been shown in CeO_2,[16] ThO_2,[17] and UO_2 (Ref. 15) that the transition has a hysteresis of approximately 20 GPa at room temperature. This hysteresis indicates the existence of a barrier in the Gibbs free energy, and it is possible that the transition pressures measured on loading at room temperature are not the equilibrium transition pressures. Such a bar-

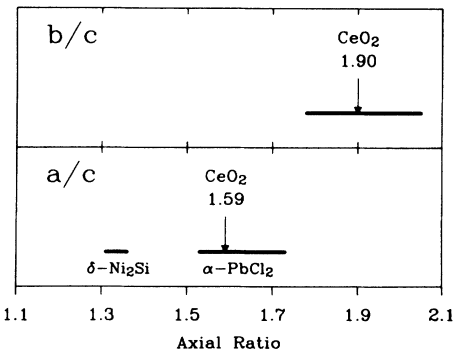

FIG. 3. The measured axial ratios for the orthorhombic *Pnam* phase relative to the range of ratios measured for materials crystallizing in the *Pnam* space group at ambient conditions (Ref. 18). The ratio *a/c* separates into δ-Ni_2Si-like and $\alpha PbCl_2$-like as shown, and CeO_2 falls within the α-$PbCl_2$-like group.

TABLE II. Systematics of the fluorite (or fluoritelike) structure to *Pnam* structure phase transition for the group-IV*B* dioxides. V_t is the volume of the fluorite unit cell at the transition to *Pnam*, and V_0 is the initial volume of the fluorite unit cell. Metal-ion radii are from Ref. 25.

Material	Metal-ion radius (Å)	P_t (GPa)	V_t/V_0
ZrO_2 [a]	0.84	16	0.89
CeO_2 [b]	0.97	31.5	0.90
UO_2 [c]	1.00	35	0.90
ThO_2 [d]	1.06	30	0.88

[a]References 11 and 12.
[b]Present work.
[c]References 14 and 15.
[d]Reference 17. $B_0=193$ GPa from ultrasonic data (Ref. 26), and $B_0'=4.00$.

rier can explain both the sluggishness of the transition, and the possibly lower transition pressure at higher temperatures as discussed in the preceding section.

CONCLUSIONS

This study has detailed the high-pressure room-temperature behavior of CeO_2, as well as clarified the general high-pressure behavior of fluorite-type dioxides. The bulk modulus of CeO_2, measured for the first time, is 230 ± 10 GPa with an assumed pressure derivative of 4.00. CeO_2 transforms on loading to an orthorhombic structure of space group *Pnam* at 31.5 ± 1.0 GPa with a fractional volume decrease of $7.5\%\pm0.7\%$. Previous Raman spectroscopy work has shown that the structure of ThO_2 above 30 GPa is the same as the CeO_2 high-pressure phase. Therefore, we have shown that this orthorhombic structure appears to be the stable postfluorite structure for all fluorite-type dioxides, independent of metal-ion size. The fractional volume at which the transition to orthorhombic occurs is 0.89 ± 0.01, thus explaining the higher transition pressures of the larger metal-ion dioxides which also have larger bulk moduli. Further work will be needed to determine the positions of the 12 atoms within the orthorhombic cell, and whether this phase is stable in postfluorite group-IV *A* dioxides such as PbO_2.

ACKNOWLEDGMENTS

We wish to thank the U.S. Department of Energy for its support through Grant No. DE-FG02-87ER45320. One of us (S.J.D.) thanks AT&T for support. We acknowledge the assistance of Keith E. Brister, Serge Desgreniers, Samuel T. Weir, and the entire CHESS staff.

[1]D. P. Dandekar and J. C. Jamieson, Trans. Am. Crystallogr. Assoc. **5**, 19 (1969).
[2]G. A. Samara, Phys. Rev. B **2**, 4194 (1970).
[3]E. D. D. Schmidt and K. Vedam, J. Phys. Chem. Solids **27**, 1563 (1966).
[4]Jane R. Kessler, Eric Monberg, and Malcolm Nicol, J. Chem. Phys. **60**, 5057 (1974).
[5]P. Boldrini and B. O. Loopstra, Acta. Crystallogr. **22**, 744 (1967).
[6]G. A. Kourouklis and E. Anastassakis, Phys. Rev. B **34**, 1233 (1986).
[7]G. A. Kourouklis and E. Anastassakis, Phys. Status Solidi B (to be published).
[8]M. Gondrand, J. C. Joubert, J. Chenavas, J. J. Capponi, and M. Perroud, Mater. Res. Bull **5**, 769 (1970).
[9]Lin-Gun Liu, J. Phys. Chem. solids **41**, 331 (1980).
[10]Lin-Gun Liu, Earth Planet. Sci. Lett. **49**, 166 (1980).
[11]S. Block, J. A. H. DaJornada, and G. J. Piermarini, J. Am. Ceram. Soc. **68**, 497 (1985).
[12]L. C. Ming and M. H. Manghnani, in *Solid State Physics under Pressure: Recent Advance with Anvil Device,* edited by S. Minomura (KTK Scientific, Tokyo, 1985), p. 135.
[13]Lin-Gun Liu and William A. Bassett, *Elements, Oxides, Silicates* (Oxford University Press, New York, 1986).
[14]T. M. Benjamin, G. Zou, H. K. Mao, and P. M. Bell, Carnegie Inst. Yearbook **80**, 280 (1981).
[15]U. Benedict, G. D. Andreetti, J. M. Fourier, and A. Waintal, J. Phys. (Paris) Lett. **43**, L171 (1982).
[16]G. A. Kourouklis, A. Jayaraman, and G. P. Espinosa, Phys. Rev. B **37**, 4250 (1988).
[17]A. Jayaraman, G. A. Kourouklis, and L. G. Van Uitert, Pramana J. Phys. **30**, 225 (1988).
[18]Ralph W. G. Wycoff, *Crystal Stuctures* (Interscience, New York, 1964), Vol. 2.
[19]H. K. Mao, P. M. Bell, J. Shaner, and D. Steinberg, J. Appl. Phys. **49**, 3276 (1978).
[20]Keith E. Brister, Yogesh K. Vohra, and Arthur L. Ruoff, Rev. Sci. Instrum. **57**, 2560 (1986).
[21]*Powder Diffraction File,* edited by W. F. McClune (JCPDS International Centre for Diffraction Data, Swarthmore, PA, 1980).
[22]F. Birch, J. Geophys. Res. **83**, 1257 (1978).
[23]Karl F. Herzfeld, J. Chem. Phys. **44**, 429 (1966); D. A. Goldhammer, *Dispersion und Absorption des Lichtes* (Tubner Verlag, Leipzig, 1913), p. 27.
[24]Wolfgang Jeitschko, Acta Crystallogr., Sec. B **24**, 930 (1968).
[25]R. D. Shannon and C. T. Prewitt, Acta. Crystallogr., Sect. B **25**, 925 (1969).
[26]P. M. Macedo, W. Capps, and J. B. Wachtman, Jr., J. Am. Ceram. Soc. **47**, 651 (1964).